ANALYSIS OF GLOBAL TIME SERIES OF CLOUD PROPERTIES FROM GOME/GOME-2 SPECTROMETERS

L. Lelli, A. A. Kokhanovsky, V. V. Rozanov, M. Vountas, and J. P. Burrows

Institute of Environmental Physics and Remote Sensing, University of Bremen
Otto-Hahn-Allee 1, 28334 Bremen, Germany
Email: luca@iup.physik.uni-bremen.de
Tel: +49 421 218 62097
Fax: +49 421 218 62070

ABSTRACT

Global long term observations of Earth atmospheric components are needed for the study of climate processes. Clouds play a prominent role also in the assessment of radiation budget and hydrological cycle. Moreover, potential trends in cloudiness can support models and forecasting. In order to achieve accurate and homogeneous time series, we analyse global retrievals of cloud properties (top height, optical thickness and albedo) derived from hyperspectral measurements of the GOME sensor family. The retrievals are obtained from top-of-atmosphere backscattered solar light in the oxygen A-band using the Semi-Analytical CloUd Retrieval Algorithm SACURA. The physical framework relies on asymptotic equations of radiative transfer. Moreover, analysis of global and regional distributions can give insights into both natural and anthropogenic signatures of large scale climate perturbations.

Key words: Cloud Top Height; Cloud Albedo; Cloud Optical Thickness; GOME; GOME-2; Radiative Transfer; Oxygen A-band.

1. INTRODUCTION

European hyperspectral satellite-based instruments started sensing the Earth back in 1996 with the Global Ozone Monitoring Experiment (GOME/ERS-2, [2]), continued with the SCanning Imaging Absorption spectroMeter for Atmospheric CartograpHY (SCIAMACHY/ENVISAT, [1]) and, at present, with the follow-on GOME-2/Metop-A [3]. In this study we will focus on the GOME instruments.
Even though the main scientific target of the spectrometers is the direct characterization of tropospheric gases, cloud properties can be derived when looking at the absorption band of oxygen. Clouds in the visible part of the electromagnetic spectrum are highly reflective, thus most of the photons do not penetrate through them, and the oxygen below the clouds is shielded. This implies that clouds at different heights will change the absorption band depth of oxygen at 761 nm (the A-band). Cloud optical thickness (COT) and cloud albedo (CA) are obtained in the continuum outside the band (i.e., at 758 nm).
The inferred cloud properties are of use to improve trace gas retrievals as well as to assess long-term climatological processes. The algorithm used in this work is the Semi-Analytical CloUd Retrieval Algorithm (SACURA, [6, 7, 14]) and the derived datasets are termed SACURA-Next Generation for GOME (SNGome), whose details and error analysis can be found elsewhere ([9, 10]). The datasets can be freely downloaded at `http://www.iup.uni-bremen.de/~sciaproc/SNGome/`.

Briefly, the algorithm works as follows: the extraction of the Earthshine radiances, the geo-referencing and the correction for degradation takes place within the GOME Data Processor v.4.0 chain [16]. They are subsequently normalised to the solar irradiance. Given the fractional cloud cover value (CF), delivered by the Optical Cloud Recognition Algorithm (OCRA, [12]), the reflectances are weighted with the Independent Pixel Approximation (IPA, [13]). In this way, we scale the actual reflectance R_{mes} to the reflectance R_{cl} generated by a full cloudy (i.e., CF = 1) and a cloud-free (i.e., CF = 0) scene with the following equation

$$R_{\text{mes}} = \text{CF}\, R_{\text{cl}} + (1 - \text{CF})\, R_{\text{sky}}. \qquad (1)$$

The clear-sky reflectance R_{sky} is substituted by the GOME Minimum Lambert-Equivalent Reflectivity (MLER), being the value taken from the global database Tropospheric Emission Monitoring Internet Service (TEMIS, [5]). Then the minimal difference between the measured R_{cl} and the forward-calculated (with the asymptotic relations of radiative transfer) spectrum is looked for along the oxygen A-band, at the nominal spectral sampling of the instruments.

At present, we have processed 7 years of GOME and 4.5 years of GOME-2 measurements (see Table 1). It has to

Proc. of 'ATMOS 2012 – Advances in Atmospheric Science and Applications',
Bruges, Belgium (ESA SP-708, November 2012)

be noted that the ERS-2 payload has been in operation until July 2011, but due to the GOME tape recorder failure and the associated loss of global coverage, no GOME data are processed after May 2003.

Table 1. Time coverage of the respective datasets.

Time window	Instrument
1996 / 06 – 2003 / 05	GOME / ERS-2
2007 / 01 – 2011 / 05	GOME-2 / Metop-A

2. DATA SELECTION

The plotting of the occurrences of the quality flags (Fig. 1 and their meaning in Tab. 2) for the two datasets (cumulatively 11.5 years) in function of cloud top height shows differences which can be explained by the different spatial resolution of the respective instruments. GOME pixel size is 320 $\times$40 km^2, whereas GOME-2 has a pixel size of 80 km $\times$ 40 km^2. This impacts the characteristics of the sensed clouds. For instance, when a vertically heterogeneous cloud scene is sensed (i.e., multi-layered scene), the algorithm retrieves unrealistic high geometrical thickness values, which, in turn, implies a bias in cloud top height and assigns quality flag 3 [10, 14]. Therefore the coarser (smaller) the ground pixel, the most (least) occurrent is flag 3. This situation is depicted in Figure 1: the green curve exhibits a second mode for CTH $>$ 9 km. In Table 3 the statistics of the quality flags for the GOME instruments are compared. We see that GOME-2 senses less heterogeneous clouds (2.11% compared to 5.69% of GOME); that the ratio of fully converged retrievals (flag 5) is more than doubled with GOME-2 measurements and that the failed retrievals (flag 0) drop from 23.88% to 6.11% of the total number of observations. These changes in the quality flagging indicate how the modeling of clouds as single-layer is better suited for better spatially resolved instruments. In the following sections we will make use of retrievals flagged 2, 3 (excluding CTH $>$ 5 km) and 5 to generate time series and global maps, which must be intended as results for single-layer clouds.

Table 2. SNGome quality flags.

Value	Description
0	No retrieval
1	Only cloud bottom height convergence
2	Only cloud top height convergence
3	Geometrical thickness limit
4	No convergence
5	Cloud top and bottom height convergence

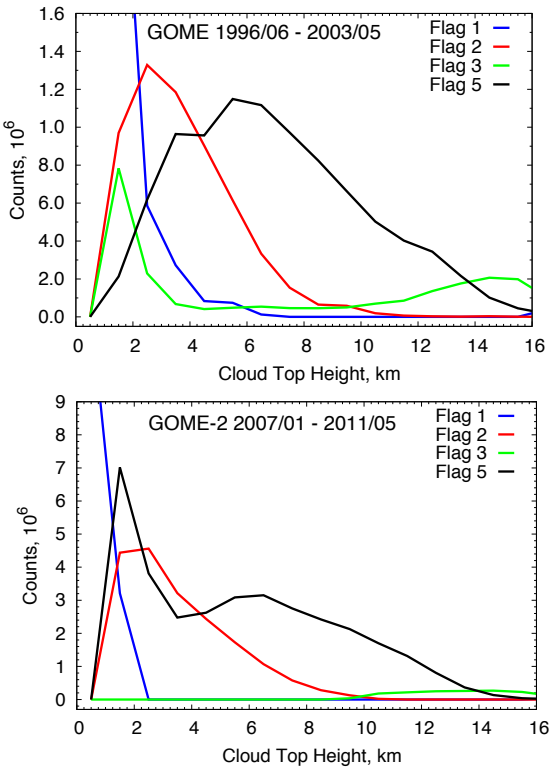

Figure 1. Quality flag counts in function of cloud top height for the 11.5 years of the SNGome datasets. The meaning of the flags is given in Table 2. The difference in the black and green curves shows the influence of the instrumental spatial resolution.

Table 3. Statistics of the quality flags for GOME (total number of observations 41,183,749) and GOME-2 (73,388,121).

Flag value	GOME (%)	GOME-2 (%)
0	23.88	6.11
1	34.6	20.51
2	13.71	25.15
3	5.69	2.11
4	0.002	0.004
5	22.10	46.1

3. TIME SERIES AND CLOUD FRACTION COMPARISON

The individual retrievals have been projected onto a rectangular equal-distance lattice of 1°$\times$ 1°side length and monthly averaged over the latitudinal belt of 70°N-70 °S. As additional step each grid block is weighted by its area, calculated as spherical triangles, in order to take into account the curvature of the globe. The resulting time series in cloud top height are plotted in Figure 2. The cloud up-

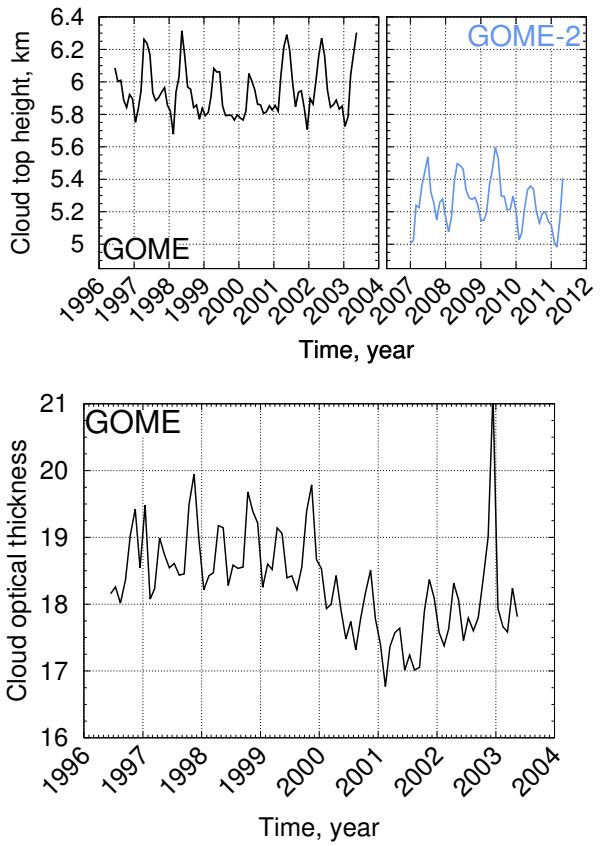

Figure 2. Monthly mean cloud top heights (upper plot) and cloud optical thickness (lower plot), averaged over 70°N-70 °S from GOME and GOME-2.

draft between GOME-2 and GOME is evident. Overall, it seems that cloud decks rise up ≈ 700 m. We think that this effect can not be explained by mere convection, due to the ≈ 60 minutes delay of overpass between GOME-2 (9:30 LT) and GOME (10:30 LT). Thus a comparison with the diurnal cycle of cloud top height as seen by geostationary satellites, for instance by the SEVIRI instrument aboard MSG platform, will help to disentangle real climatological effects from specific instrumental calibration/degradation issues.

In addition, we have processed 3.5 years (January 2007 - May 2010) of GOME-2 measurements and retrieved cloud top heights with the cloud fraction (and surface albedo) calculated with the FRESCO algorithm [18] and plotted in Figure 3 together with the same record processed with OCRA cloud fraction. Clearly the two datasets are different in the total number of pixels, but the calculation of monthly means smooths short-term oscillations, making this comparison valuable. Firstly, there is a systematic bias of ≈ 650 m for the whole period. Secondly, the CTH/OCRA dataset displays different features, especially in late winter-early spring months and in summer months. Overall the seasonality is preserved in both datasets.

Understanding the reasons for this offset is not a straightforward task, due to the presence, in the framework of the independent pixel approximation, of surface contributions as well as clear-sky signals and owing to the two different approaches to infer CF values. OCRA is a color space algorithm, which uses broadband polarisation measurements, whereas FRESCO employs a threshold method and assumes clouds as perfect Lambertian reflectors with fixed albedo equal to 0.8.

In view of Eq. 1, the depth of the oxygen A-band seen by the sensor depends on cloud fraction. Therefore we plot the zonally averaged ratio of FRESCO CF to OCRA CF in Figure 4. The figure shows a seasonally dependent underestimation (up to a factor of 2) of FRESCO as compared to OCRA in the belt of 15°N - 5 °S. Starting from March 2008 onward, FRESCO cloud fraction slowly approaches OCRA values at almost all latitudes, except in the tropics.

The influence of CF discrepancies can be seen in Figure 5, where the timeseries of Figure 3 are zonally averaged and compared. The patterns of FRESCO CF underestimation (or OCRA CF overestimation) correlate with SNGome CTH/FRESCO underestimation (or CTH/OCRA overestimation). In the sub-tropical belts (at ≈ 20°N and ≈ 20°S) and in the relative boreal and austral winters, the white spots indicate a general agreement between the two datasets and the ratio FRESCO CF / OCRA CF → 1.

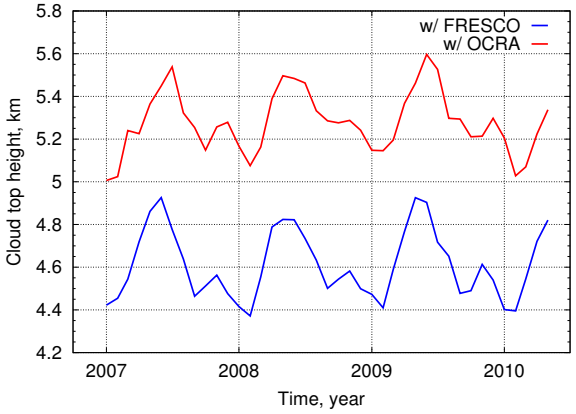

Figure 3. Monthly mean cloud top heights from GOME-2, averaged over 70°N-70 °S, calculated with OCRA (red curve) and FRESCO (blue curve) cloud fraction.

4. ZONAL ANALYSIS

Figures 6 and 7 depict the zonally averaged timeseries of cloud top height and optical thickness, respectively. Examining Fig. 6, the typical features of cloudiness are represented in both GOME and GOME-2 datasets for cloud top height: the seasonality of the equatorial maximum placement, the steady marine boundary layer clouds in the belt 10°S - 30 °S, and the decrease of the tropopause height in the high latitudinal belts, among others. The GOME record exhibits a slightly higher variability than

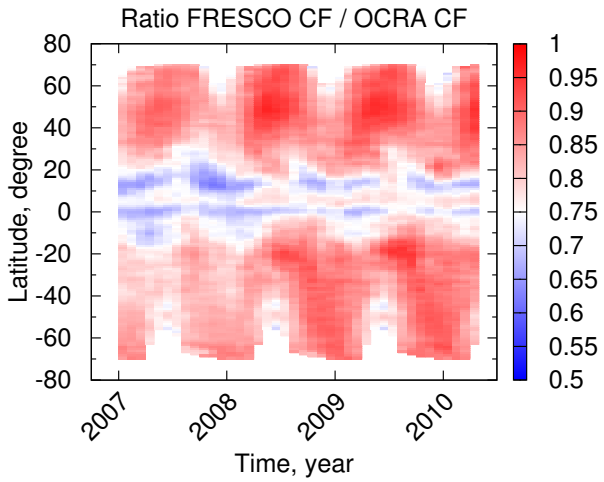

Figure 4. Monthly zonal mean ratios between FRESCO cloud fraction and OCRA cloud fraction, both derived from GOME-2 measurements.

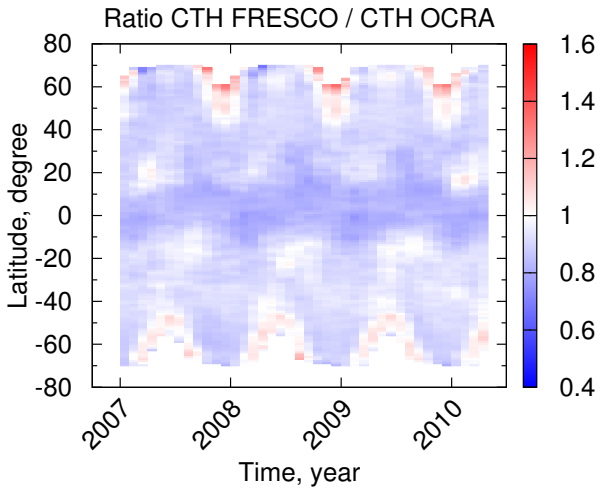

Figure 5. Monthly zonal mean ratios between SNGome cloud top height calculated with FRESCO cloud fraction to SNGome cloud top height calculated with OCRA cloud fraction, both derived from GOME-2 measurements.

GOME-2. The same plot for optical thickness (not shown here) reveals a systematic offset between the two instruments. Moreover, between February and March 2008, a leap is visible for all latitudes, which can be related to a change in the Polarisation Measuring Device (PMD) band definition [4], which impacts the retrieval of optical thickness through the determination of cloud fraction and, eventually, of the cloud reflection function R_{cl} in Eq. 1. This effect is currently being assessed.

However this bias is absent in the CTH record. This is a consequence of the fact that CTH is retrieved iteratively along the oxygen absorption band, using 67 spectral points, with reflectances normalised to their value at 758 nm. Conversely COT is calculated using a single-channel algorithm at 758 nm and only absolute radiance values are used, thus affecting COT retrievals.

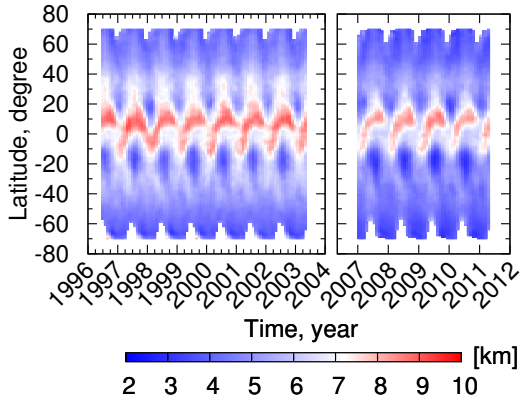

Figure 6. Zonal monthly means of cloud top height from GOME and GOME-2, averaged over all longitudes.

5. GLOBAL MAPS

Figures 8 and 9 show global maps of cloud top heights retrieved by GOME and GOME-2, respectively. Figure 10 shows cloud optical thickness derived from GOME. As can be seen in Figure 10, some regions, known to be covered by snow, are misinterpreted as thick clouds. This is due to missing contrast between very bright surfaces and clouds, which are both reflective in the visible wavelengths. Moreover it has to be noted that, at the present stage, our algorithm can not distinguish the thermodynamic phase of water. The GOME spectrometers are not equipped with SWIR channels, which would make feasible the retrieval of single scattering albedo, thus enabling the calculation of phase function and actual size of droplets and/or ice crystals. Therefore one must assume the microphysical parameters of water from the very beginning, which may lead to errors in the retrievals.

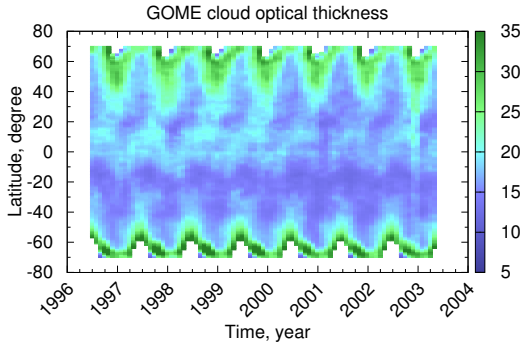

Figure 7. Zonal monthly means of cloud optical thickness from GOME, averaged over all longitudes.

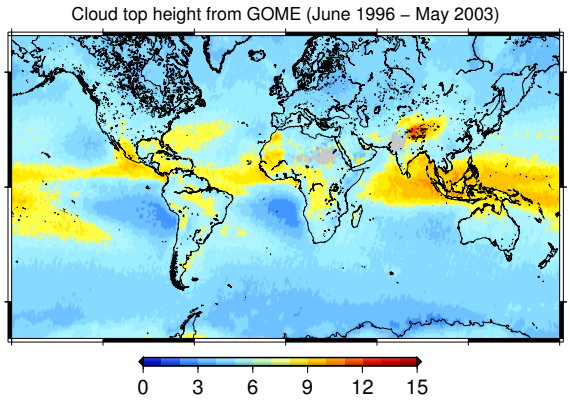

Figure 8. Global cloud top heights from GOME.

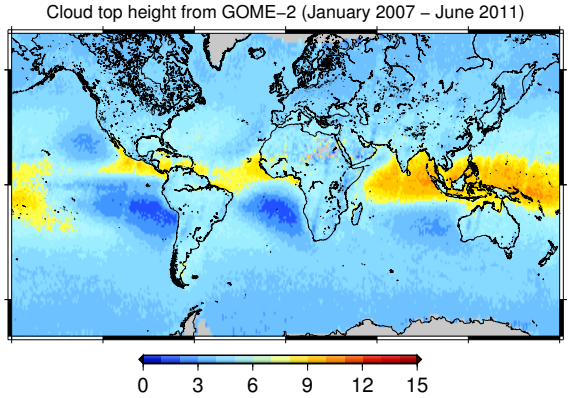

Figure 9. Global cloud top heights from GOME-2.

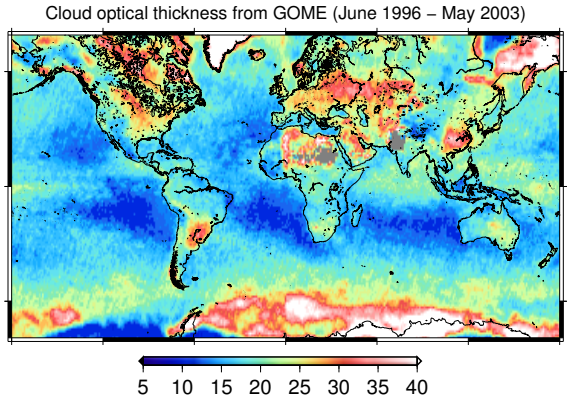

Figure 10. Global cloud optical thickness from GOME.

6. SUMMARY AND OUTLOOK

We have processed and intercompared 11.5 years of cloud top height and cloud optical thickness derived by GOME and GOME-2 measurements in the oxygen A-band. The applied algorithm relies on the asymptotic relations of radiative transfer and is valid for warm water clouds of optical thickness > 5. Firstly, the better spatial resolution of GOME-2 has lead to a significant improvement of the algorithm performance. Secondly, the inspection of time-series of derived cloud parameters shows biases between GOME and GOME-2. Such offsets can be addressed if looking at surface pressures in the oxygen A-band for a clear-sky atmosphere [17] or choosing one reference sensor and applying a two-step spatio-temporal correction [11].

The cloud top height dataset is less (or not at all) affected by these biases due to the multiple channel algorithm employed, but depends on the auxiliary cloud fraction dataset used anyway. The spatial and temporal patterns of discrepancies between FRESCO cloud fraction and OCRA cloud fraction, when compared to differences in the retrieved cloud altitudes, suggest that the two cloud fraction algorithms are climatology dependent, that is, only certain cloud types are (not) well captured. This behavior leaves room for improvements in the detection of the fractional cloud cover and makes desirable the approach of the synergetic calculation of geometrical cloud cover from two different instruments aboard the same platform, when sensing the same scene. This method has been already applied to SCIAMACHY and MERIS radiances aboard ENVISAT [8, 15] and can be replicated for the combinations GOME / ATSR-2 and GOME-2 / AVHRR-3.

ACKNOWLEDGMENTS

We thank ESA and DLR for providing the data. EUMETSAT is credited for making GOME-2 radiances available. Generic Mapping Tools (GMT) and Climate Data Operators (CDO) were used for this work.

REFERENCES

[1] Bovensmann, H., Burrows, J. P., Buchwitz, M., Frerick, J., Noël, S., Rozanov, V. V., Chance, K. V., and Goede, A. P. H. (1999). SCIAMACHY: Mission objectives and measurement modes. *J. Atmos. Sci.*, 56(2):127–150.

[2] Burrows, J. P., Weber, M., Buchwitz, M., Rozanov, V. V., Ladsttätter Weissenmayer, A., Richter, A., DeBeek, R., Hoogen, R., Bramstedt, K., Eichmann, K. U., Eisinger, M., and Perner, D. (1999). The Global Ozone Monitoring Experiment (GOME): Mission Concept and First Scientific Results. *J. Atmos. Sci.*, 56:151–175.

[3] Callies, J., Corpaccioli, E., Eisinger, M., Hahne, A., and Lefebvre, A. (2000). GOME-2- Metop's second-generation sensor for operational ozone monitoring. *ESA bulletin*, 102:28–36.

[4] EUMETSAT (2010). GOME-2 PMD Band Definitions 3.0 and PMD Calibration. Technical Report EUM/OPS-EPS/DOC/07/0601, EUMETSAT, Darmstadt, Germany.

[5] Koelemeijer, R. B. A., de Haan, J. F., and Stammes, P. (2003). A database of spectral surface reflectivity in the range 335-772 nm derived from 5.5 years of GOME observations. *J. Geophys. Res.*, 108:4070. `http://www.temis.nl/data/ler.html`.

[6] Kokhanovsky, A. A. and Nauss, T. (2006). Reflection and transmission of solar light by clouds: asymptotic theory. *Atmos. Chem. Phys.*, 6:5537–5545.

[7] Kokhanovsky, A. A. and Rozanov, V. V. (2004). The physical parameterization of the top-of-atmosphere reflection function for a cloudy atmosphere–underlying surface system: the oxygen A-band case study. *J. Quant. Spectrosc. Rad. Trans.*, 85(1):35–55.

[8] Kokhanovsky, A. A., von Hoyningen-Huene, W., and Burrows, J. P. (2009). Determination of the cloud fraction in the SCIAMACHY ground scene using MERIS spectral measurements. *Int. J. Rem. Sens.*, 30(23):6151–6167.

[9] Lelli, L., Kokhanovsky, A. A., Rozanov, V. V., and Burrows, J. P. (2011a). Radiative transfer in the oxygen A-band and its application to cloud remote sensing. *Atti Acc. Pel. Per.*, 89(S1):C1V89S1P056–1–C1V89S1P056–4.

[10] Lelli, L., Kokhanovsky, A. A., Rozanov, V. V., Vountas, M., Sayer, A. M., and Burrows, J. P. (2011b). Seven years of global retrieval of cloud properties using space-borne data of GOME. *Atmos. Meas. Tech. Discuss.*, 4(4):4991–5035.

[11] Loyola, D. G., Coldewey-Egbers, R. M., Dameris, M., Garny, H., Stenke, A., Van Roozendael, M., Lerot, C., Balis, D., and Koukouli, M. (2009). Global long-term monitoring of the ozone layer - a prerequisite for predictions. *Int. J. of Rem. Sens.*, 30(15-16):4295–4318.

[12] Loyola, D. G. and Ruppert, T. (1998). A new PMD cloud-recognition algorithm for GOME. *ESA Earth Observation Quarterly*, 58:45–47.

[13] Marshak, A., Davis, A., Wiscombe, W., and Titov, G. (1995). The verisimilitude of the independent pixel approximation used in cloud remote sensing. *Rem. Sens. Environ.*, 52(1):72–78.

[14] Rozanov, V. V. and Kokhanovsky, A. A. (2004). Semianalytical cloud retrieval algorithm as applied to the cloud top altitude and the cloud geometrical thickness determination from top-of-atmosphere reflectance measurements in the oxygen A-band. *J. Geophys. Res.*, 109:4070.

[15] Schlundt, C., Kokhanovsky, A. A., von Hoyningen-Huene, W., Dinter, T., Istomina, L., and Burrows, J. P. (2011). Synergetic cloud fraction determination for SCIAMACHY using MERIS. *Atmos. Meas. Tech.*, 4(4):319–337.

[16] Slijkhuis, S. and Loyola, D. G. (2009). GOME Data Processor (GDP), Extraction Software and User's Manual. Technical Report ER-SUM-DLR-GO-0045, DLR, Oberpfaffenhofen, Germany.

[17] van Diedenhoven, B., Hasekamp, O. P., and Aben, I. (2005). Surface pressure retrieval from SCIAMACHY measurements in the O_2 A-band: validation of the measurements and sensitivity on aerosols. *Atmos. Chem. Phys.*, 5(8):2109–2120.

[18] Wang, P., Stammes, P., van der A, R., Pinardi, G., and van Roozendael, M. (2008). FRESCO+: an improved O_2 A-band cloud retrieval algorithm for tropospheric trace gas retrievals. *Atmos. Chem. Phys.*, 8(21):6565–6576.